Supporting Information

Construction of 2D zinc(II) MOFs with tricarboxylate and *N*-donor mixed ligands for multiresponsive luminescence sensor and CO_2 adsorption

Kenika Khotchasanthong,[a] Kunlanit Chinchan,[a] Kanokwan Kongpatpanich,[b] Waraporn Pinyo,[c] Filip Kielar,[d] Winya Dungkaew,[e] Mongkol Sukwattanasinitt,[f] Sakchai Laksee,[g] and Kittipong Chainok*[a,h]

[a]Thammasat University Research Unit in Multifunctional Crystalline Materials and Applications (TU-MCMA), Faculty of Science and Technology, Thammasat University, Pathum Thani 12121, Thailand, E-mail: kc@tu.ac.th; Fax: +662 654 4548; Tel: +66 86 339 5079

[b]School of Molecular Science and Engineering, Vidyasirimedhi Institute of Science and Technology, Rayong 21210, Thailand

[c]NSTDA Characterization and Testing Center, Thailand Science Park, Pathum Thani 12120, Thailand

[d]Department of Chemistry, Faculty of Science, Naresuan University, Phitsanulok 65000, Thailand

[e]Department of Chemistry, Faculty of Science, Mahasarakham University, Maha Sarakham 43100, Thailand

[f]Department of Chemistry, Faculty of Science, Chulalongkorn University, Bangkok 10330, Thailand

[g]Nuclear Technology Research and Development Center, Thailand Institute of Nuclear Technology (Public Organization), Ongkharak, Nakhon Nayok, 26120, Thailand

[h]Center of Excellence on Petrochemical and Materials Technology, Chulalongkorn University, Bangkok 10330, Thailand

Table S1 Crystallographic data and refinement summary for **1** and **2**.

Compound (CCDC No.)	**1 (2363871)**	**2 (2363872)**
Empirical formula	$C_{67}H_{62}N_7O_{13}Zn_2$	$C_{69}H_{71}N_8O_{16}Zn_2$
Formula weight	1302.96	1399.07
Temperature (K)	100(2)	100(2)
Crystal system	Monoclinic	Triclinic
Space group	$P2_1/n$	P-1
a (Å)	16.3834(5)	14.5880(4)
b (Å)	27.2898(9)	16.0895(4)
c (Å)	17.2612(6)	16.5097(4)
α (°)	90	65.0510(10)
β (°)	112.9720(10)	86.8360(10)
γ (°)	90	89.4830(10)
V (Å^3)	7105.4(4)	3507.66(16)
D_{calc} (g cm^{-3})	1.218	1.325
Z	4	2
μ (mm^{-1})	1.340	1.430
Reflections collected	76405	42959
Unique Reflections	13441	13708
R_1, wR$_2$ ($I > 2\sigma(I)$)	0.0660, 0.1885	0.0608, 0.1957
R_1, wR$_2$ (all data)	0.0716, 0.1945	0.0643, 0.2010
GOF on F^2, S	1.038	1.043
$\Delta\rho_{max}$, $\Delta\rho_{min}$ (e Å^{-3})	2.96, –0.88	1.60, –0.55

Table S2 Selected bond lengths and bond angle (Å, °) for **1** and **2**.

	1		**2**
Zn1−O1	1.996(2)	Zn1−O1	1.946(2)
Zn1−O7	1.977(2)	Zn1−O3^{i}	1.9650(19)
Zn1−O12^{i}	1.981(2)	Zn1−O6^{ii}	1.951(2)
Zn1−N1	2.005(3)	Zn1−N1	2.095(3)
Zn2−O3	1.964(2)	Zn2−O7	1.968(2)
Zn2−O5^{ii}	1.968(2)	Zn2−O10^{iii}	1.9893(19)
Zn2−O9^{iii}	2.028(2)	Zn2−O11^{iv}	2.124(3)
Zn2−N3	2.041(2)	Zn2−O12^{iv}	2.188(2)
O1−Zn1−N1	121.64(10)	Zn2−N2	2.130(3)
O7−Zn1−O1	101.32(9)	O1−Zn1−O3^{i}	130.52(9)
O7−Zn1−O12^{i}	129.34(9)	O1−Zn1−O6^{ii}	120.47(9)
O7−Zn1−N1	95.99(10)	O1−Zn1−N1	101.07(10)
O12^{i}−Zn1−O1	100.23(9)	O3^{i}−Zn1−N1	100.57(10)
O12^{i}−Zn1−N1	110.35(10)	O6^{ii}−Zn1−O3^{i}	101.37(9)
O3−Zn2−O5^{ii}	123.55(9)	O6^{ii}−Zn1−N1	94.61(12)
O3−Zn2−O9^{iii}	118.59(9)	O7−Zn2−O10^{ii}	103.79(10)
O5^{ii}−Zn2−O9^{iii}	99.80(9)	O7−Zn2−O11^{iv}	109.97(10)
O3−Zn2−N3	100.43(9)	O7−Zn2−O12^{iv}	112.12(10)
O5^{ii}−Zn2−N3	116.45(10)	O7−Zn2−N2	91.74(11)
O9^{iii}−Zn2−N3	95.18(9)	O10^{iii}−Zn2−O11^{iv}	144.30(10)
		O10^{iii}−Zn2−O12^{iv}	96.85(9)
		O10^{iii}−Zn2−N2	92.27(9)
		O11^{iv}−Zn2−O12^{iv}	59.99(10)
		O11^{iv}−Zn2−N2	97.90(10)
		N2−Zn2−O12^{iv}	151.37(11)

Symmetry codes: (i) $x-1, y, z$; (ii) $x+1, y, z$; (iii) $x, y-1, z$; (iv) $x, y+1, z$ for **1**;
(i) $x, y-1, z$; (ii) $x, y, z-1$; (iii) $x, y+1, z-1$; (iv) $x, y+1, z$ for **2**.

Table S3 Examples of Zn-based MOF luminescent sensors for metal ion detection.

Zn-based MOFs	Ions	K_{sv} (M^{-1})	LOD	Ref
$[Zn_2(L^1)_2(bpp)(H_2O)_2]$	Fe^{3+}	1.68×10^4	1.76 μM	1
	Hg^{2+}	1.34×10^4	3.75 μM	1
$[ZnL^2(dpa)]$	Fe^{3+}	3.09×10^4	1.94 μM	2
HBU-19	Fe^{3+}	2.24×10^5	3.40 μM	3
TMU-16	Fe^{3+}	2.80×10^4	20.0 μM	4
TMU-48	Fe^{3+}	1.86×10^5	1.79 μM	5
$[Zn(BBDF)(ATP)]\cdot 2DMF\cdot 3H_2O$	Hg^{2+}	3.89×10^4	0.12 μM	6
$[Zn(TIBTC)(DMA)](Me_2NH_2)$	Fe^{3+}	9.71×10^4	6.40 μM	7
$[Zn_2(tpeb)(bpdc)_2](Me_2NH_2)_{0.5}\cdot 4H_2O$	Fe^{3+}	1.33×10^4	0.88 μM	8
$[Zn_2(NO_3)_2(4,4'\text{-bpy})_2(TBA)]$	Fe^{3+}	7.48×10^3	7.18 μM	9
$[Zn(5\text{-AIP})(Ald\text{-}4)]\cdot H_2O$	Fe^{3+}	9.00×10^4	0.30 μM	10
	Cr^{3+}	2.30×10^4	0.46 μM	
[Zn(tbda)]	Cr^{3+}	2.68×10^4	180 μM	11
$[Me_2NH_2]_4[Zn_6(qptc)_3(trz)_4]\cdot 6H_2O$	Cr^{3+}	4.39×10^4	1.00 μM	12
$[Zn(L^5)(H_2O)]\cdot H_2O$	Cr^{3+}	2.03×10^4	2.44 μM	13
$[Zn_2(tbta)(phen)(OH)]\cdot 4H_2O$	Cr^{3+}	1.44×10^5	0.18 μM	14
	Cu^{2+}	2.01×10^5	0.07 μM	
$[Zn_2(L^6)(phen)(H_2O)_3]\cdot 2.4H_2O$	Cu^{2+}	4.38×10^5	134 μM	15
$[Zn(bpy)(H_2O)_4][Zn(H_2L^6)_2(bpy)(H_2O)_2]$	Cu^{2+}	7.29×10^4	33.1 μM	
$[Zn_2(5\text{-AIA})_2(DPTTZ)]\cdot DMF$	Hg^{2+}	4.20×10^4	2.17 μM	16
$[Zn(4\text{-pzpt})_2(H_2O)]$	Hg^{2+}	1.09×10^3	26.70 μM	17
$[Zn(4\text{-pzpt})_2]\cdot CH_3OH$	Hg^{2+}	7.13×10^2	34.08 μM	
ZU-1	Hg^{2+}	7.50×10^8	3.00 μM	18
MOF-5-NH_2	Cu^{2+}	-	0.06 μM	19
	Pb^{2+}	2.8×10^2	0.25 μM	
$[Zn(HPydc)_2]\cdot 2H_2O$	Pb^{2+}	5.47×10^2	5.15 μM	20
[Zn-APT]	Fe^{2+}	1.90×10^4	0.12 μM	21
$[Zn(ATA)(L^7)]\cdot H_2O$	Fe^{3+}	0.56×10^3	3.76 μM	22
	Pb^{2+}	4.18×10^4	0.20 μM	
$[Zn(OBA)(DPT)_{0.5}]\cdot DMF$	Hg^{2+}	3.74×10^3	1.80 μM	23
$[Zn(2\text{-}NH_2bdc)(bibp)]$	Hg^{2+}	4.55×10^3	42.0 μM	24
$[Zn_2(suc)_2(4\text{-nvp})_2]$	Pb^{2+}	3.80×10^5	0.05 μM	25
$[Zn(fum)(4\text{-nvp})_2]\cdot 2H_2O$	Pb^{2+}	8.22×10^5	0.13 μM	26
$[Zn(mes)(4\text{-nvp})_2]\cdot H_2O$	Pb^{2+}	5.04×10^5	0.15 μM	
[Zn(glu)(4-nvp)]	Pb^{2+}	4.90×10^5	0.15 μM	

[Zn(dttp)(H_2O)]	Cu^{2+}	4.01×10^3	250 μM	27
[$Zn_3(L^8)_2(dpp)_2$]	Cu^{2+}	9.70×10^3	1.05 μM	28
Compound **1**	Fe^{3+}	2.08×10^4	1.23 μM	This work
	Fe^{2+}	1.44×10^4	1.97 μM	This work
	Cu^{2+}	8.89×10^4	3.60 μM	This work
	Cr^{3+}	5.55×10^3	3.50 μM	This work
	Pb^{2+}	5.40×10^3	3.20 μM	This work
	Hg^{2+}	8.02×10^3	4.17 μM	This work
Compound **2**	Fe^{3+}	1.86×10^4	1.29 μM	This work
	Fe^{2+}	1.00×10^4	1.45 μM	This work
	Cu^{2+}	6.26×10^4	3.21 μM	This work
	Cr^{3+}	6.89×10^3	2.92 μM	This work
	Pb^{2+}	1.45×10^4	1.47 μM	This work
	Hg^{2+}	2.98×10^3	3.96 μM	This work

bpp = 1,3-di(4-pyridyl)propane and; H_2L^1 = 2,5-thiophenedicarboxylic acid ; H_2L^2 = 4,4′-(ethynylimino)bis[benzoic acid]; dpa = 4,4′-dipyridylamine; L^3 = 2,3,5,6-tetra(4-carboxyphenyl)pyrazine; L^4 = 1,2-di(4-pyridyl)ethylene; BBDF = 2,7-bis(1*H*-benzimidazol-1-yl)-9,9-dimethyl-9*H*-fluorene); 3,5-H_2btc = 1,3,5-benzenetricarboxylic acid; DAT = diamino triazole; H_2ATP = 2-aminoterephthalic acid; H_3TIBTC = 2,4,6-triiodo-1,3,5-benzenetricarboxylic acid; DMA = dimethylacetamide; H_2tpeb = 1,3,5-tri-4-pyridyl-1,2-ethenylbenzene; H_2bpdc = biphenyl-4,4′-dicarboxylic acid; H_2TBA = 4-(1*H*-tetrazol-5-yl)-benzoic acid; 4,4′-bpy = 4,4′-bipyridine; 5-AIP = 5-amino isophthalate; Ald-4 = aldrithiol-4; H_2tbda = 4-(2,2′;6′,2″-tripyridyl)-4′-1,2-phenyl dicarboxylic acid; H_4qptc = terphenyl-2,5,2′5′-tetracarboxylic acid; trz = 1,2,4-triazole; H_2L^5 = 5-(2- methylpyridin-4-yl)isophthalic acid; H_3tbta = 1-(triazol-1-yl)- 2,4,6-benzene tricarboxylic acid; phen = 1,10-phenanthroline; H_4L^6 = (3,5-di(3,4-dicarboxylphenyl) pyridine); 2,2-bpy = 2,2-bipyridine; 5-AIA = 5-aminoisophthalic acid; DPTTZ = N,N′-di(4-pyridyl)-thiazolo-[5,4-d]thiazole; DMF = N,N′-dimethylformamide; 4-Hpzpt = 3-(pyridin-4-yl)-5-(pyrazin-2-yl)- 1H-1,2,4-triazole; H_2ndc = 1,4-Naphthalenedicarboxylic acid; H_2Pydc = 2,3-Pyridinedicarboxylic acid; APT = 2-amino-6-purinethiol; TPC_4A = 2,8,14,20-tetra-phenyl-6,12,18,24-tetra-methoxy-4,10,16,22-tetra-carboxy-methoxy-resorcin[4]arene; TNC_4A = 2,8,14,20-tetra-1-naphthal-6,12,18,24-tetra- methoxy-4,10,16,22-tetra-carboxy-methoxy-resorcin[4]arene; L^7 = bipyridyl-based Schiff base, (*E*)-*N*′-(pyridin-4-ylmethylene)isonicotinohydrazide; H_2ATA = amino functionalized 2-aminoterephthalic acid; H_2OBA = 4,4′-oxybis(benzoic acid); DPT = 3,6-di(pyridin-4-yl)-1,2,4,5-tetrazine; 2-NH_2bdc = 2-amino-1,4-benzenedicarboxylic acid; bibp = 4,4′-bis(imidazol-1-ylmethyl)biphenyl; H_2suc = succinic acid; 4-nvp = 4-(1-naphthylvinyl)pyridine; H_2fum = fumaric acid; 4-nvp = 4-(1-naphthylvinyl)pyridine; H_2mes = mesaconic acid; H_2glu = glutaric acid; H_2 dttp = 2,5-di(1H-1,2,4-triazol-1-yl)terephthalic acid; L^8 = (3,5-dibromosalicylaldehyde salicylhydrazone); dpp = 1,3-di(4-pyridyl)propane; H_2tpt = 2,4,6-tri(pyridin-4-yl)-1,3,5-triazine; H_2tdc = 2,5-thiophenedicarboxylic acid.

Referances

1. J. Huang, X.-Y. Pu, Z. Liu, X.-Y. Cao and J. Fu, *J. Inorg. Organomet. Polym. Mater.*, 2021, **31**, 2209–2217.
2. B. Zhao, J. Lu, H. Liu, S. Li, Q. Sun and B. Zhang, *CrystEngComm*, 2024, **26**, 1319–1327.
3. J.-M. Liu, Y.-B. Ren, H.-Y. Xu, L.-J. Li, Y.-J. Mu and J.-L. Du, *Inorg. Chim. Acta*, 2021, **527**, 120583–120588.
4. Y. D. Farahani and V. Safarifard, *J. Solid State Chem.*, 2019, **275**, 131–140.
5. L. Esrafili, M. Gharib and A. Morsali, *New J. Chem*., 2019, **43**, 18079–18091.
6. C. Li, X. Sun, X. Meng, D. Wanga and C. Zheng, *Dalton Trans*., 2023, **52**, 7611–7619.
7. C. H. Liu, Q. L. Guan, X. D. Yang, F. Y. Bai, L. X. Sun and Y. H. Xing, *Inorg. Chem*., 2020, **59**, 8081–8098.
8. B. B. Rath and J. J. Vittal, *Inorg. Chem.*, 2020, **59**, 13, 8818–8826.
9. X. Zhang, X. R. Zhuang, N. X. Zhang, C. Y. Ge, X. Luo, J. X. Li, J. Wu, Q. F. Yang and R. Liu, *CrystEngComm*, 2019, **21**, 1948–1955.
10. P. Daga, P. Manna, P. Majee, D. K. Singha, S. Hui, A. K. Ghosh, P. Mahata and S. K. Mondal, *J. Inorg. Organomet. Polym. Mater.*, 2020, **30**, 4496–4509.
11. X. Liang, Y. Jia, Z. Zhan and Ming Hu, *Appl. Organometal. Chem.*, 2019, **33**, 1–11.
12. X.-X. Jia, R.-X. Yao, F.-Q. Zhang and X.-M. Zhang, *Inorg. Chem*., 2017, **56**, 2690–2696.
13. X.-Y. Guo, F. Zhao, J.-J. Liu, Z.-L. Liu and Y.-Q. Wang, *J. Mater. Chem. A*, 2017, **5**, 20035–20043.
14. X. Chen, L. Shang, H. Cui, H. Yang, L. Liu, Y. Ren and J. Wang, *CrystEngComm*, 2020, **22**, 5900–5913.
15. X. Liu, Y. Liu, S. Feng and L. Lu, *J. Mol. Struc.,* 2023, **1274**, 134570–134578.
16. A. Nath, G. M Thomas, S. Hans, S. R. Vennapusa and S. Mandal, *Inorg. Chem*., 2022, **61**, 2227–2233.
17. Y.-M. Fang, X. Ye, L. Xia, W.-W. Dong, J. Zhao and D.-S. Li, *J. Solid State Chem.*, 2018, **266**, 181–188.
18. M. S. Khan, S. Kamal, M. Zulkiflain, M. Khalid, S. Khan, M. Shahid, and M. Ahmad, *J. Mol. Liq,* 2024, **405**, 125019–125027.
19. X. An, Q. Tan, S. Pan, H. Liu, X. Hu, *Spectrochim. Acta A Mol. Biomol. Spectrosc.*, 2021, **247**, 119073–119083.
20. M. Ashafaq, M. Khalid, M. Raizada, M. S. Ahmad, M. S. Khan, M. Shahid and M. Ahmad, *J. Inorg. Organomet. Polym. Mater*, 2020, **30**, 4496–4509.
21. J. Wang, D. Yan, and W. Huang, *Inorg. Chem. Comm.*, 2022, **138**, 109282–109290.
22. B. Parmar, Y. Rachuri, K. K. Bisht and E. Suresh, *Inorg. Chem.*, 2017, **56**, 10939–10949.
23. S. A. A. Razavi, M. Y. Masoomi and A. Morsali, *Inorg. Chem.*, 2017, **56**, 16, 9646–9652.
24. L. Wen, X. Zheng, K. Lv, C. Wang and X. Xu, *Inorg. Chem*., 2015, **54**, 7133–7135.
25. S. Bera, B. Dutta, D. Mandal, C. Sinha and M. H. Mir, *Inorg. Chem*., 2022, **61**, 13244–13249.
26. B. Dutta, S. Bera, G. Bairy, M. Shit, S. Khanra, C. Sinha and M. H. Mir, *ES Energy Environ.,* 2022, **16**, 74–81.
27. H. Cai, N. Li, Y. Li and D.-M. An, *Inorg. Chim. Acta*, 2020, **512**, 119886–119891.
28. Y. Wu, Z. Gu, W. Luo, L. Wu, Y. Li, B. Xie and L. Zou, *Transit. Met. Chem.*, 2018, **43**, 673–681.

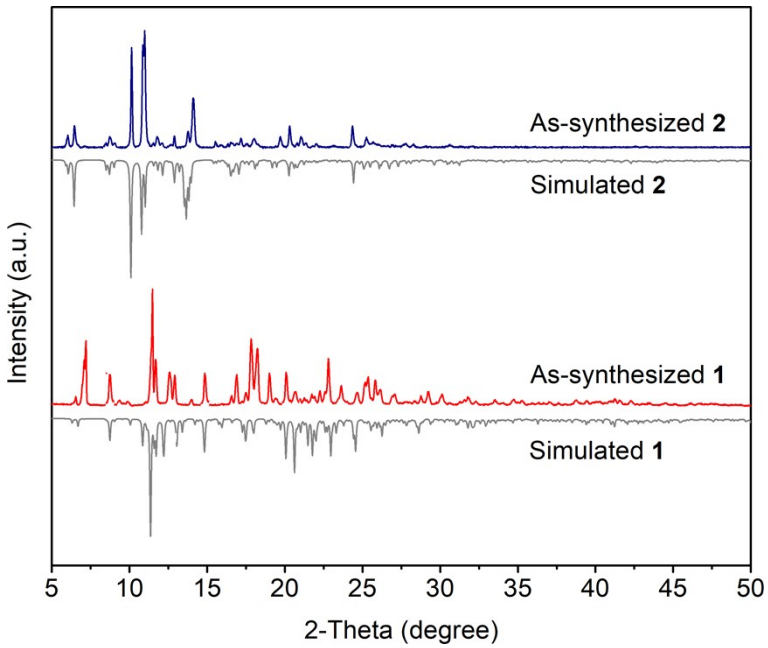

Fig. S1 Comparison of the simulated and as-synthesized PXRD patterns for **1** and **2**.

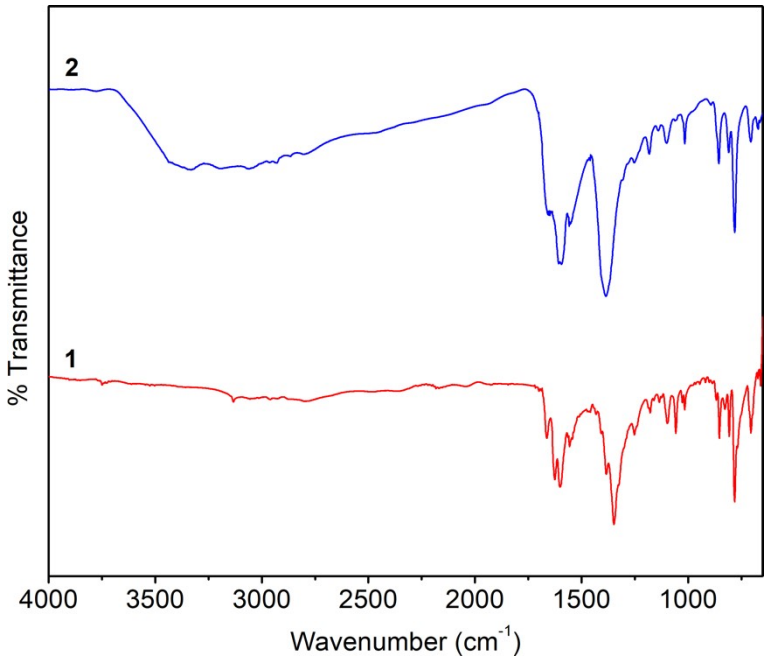

Fig. S2 The IR spectra of **1** and **2**.

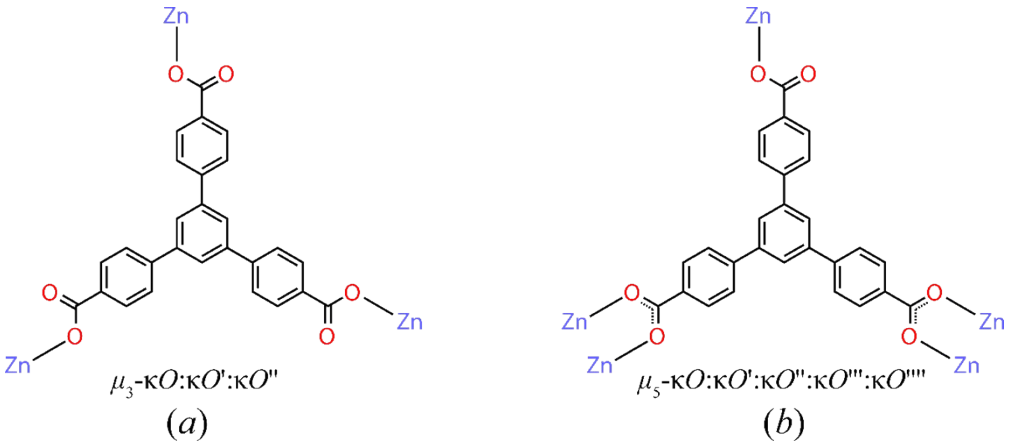

Fig. S3 The coordination modes of the btb^{3-} ligands observed in **1** and **2**.

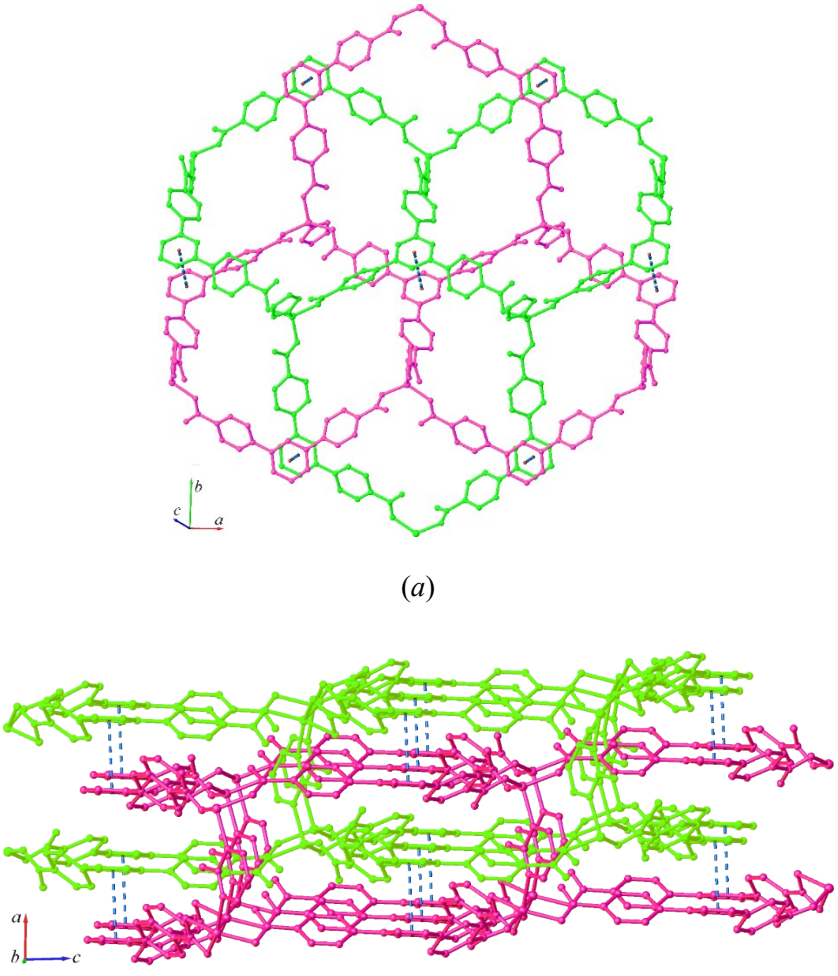

Fig. S4 Views of π···π stacking between neighboring btb^{3-} ligands for (*a*) **1** and (*b*) **2**.

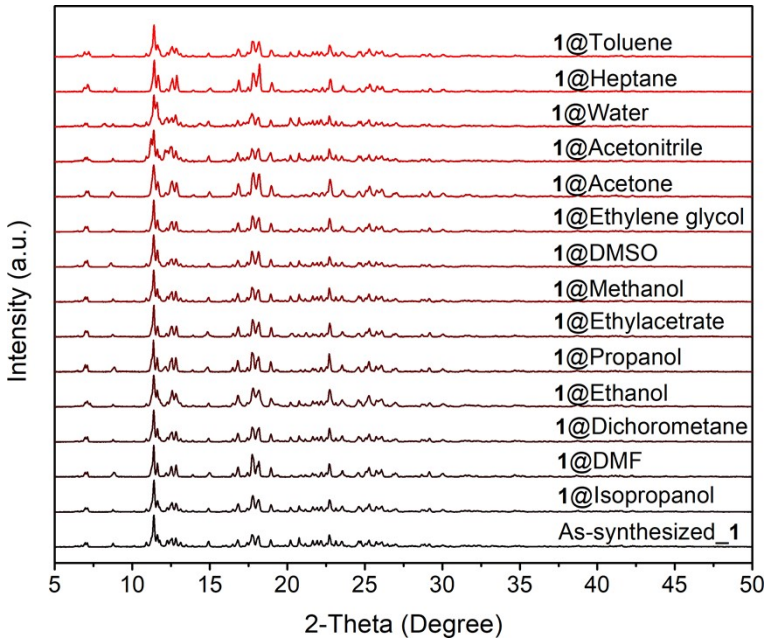

(*a*)

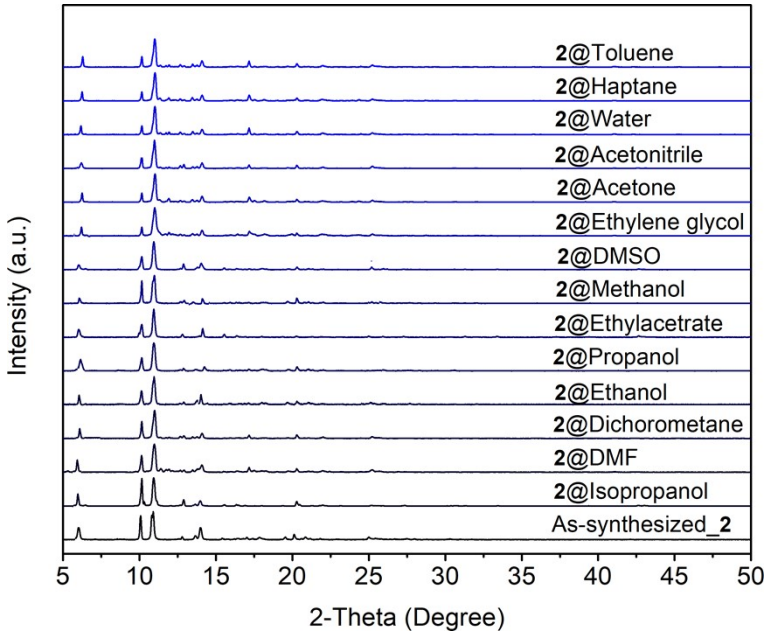

(*b*)

Fig. S5 Room temperature PXRD patterns after two days of immersion in water and various organic solvents for (*a*) **1** and (*b*) **2**.

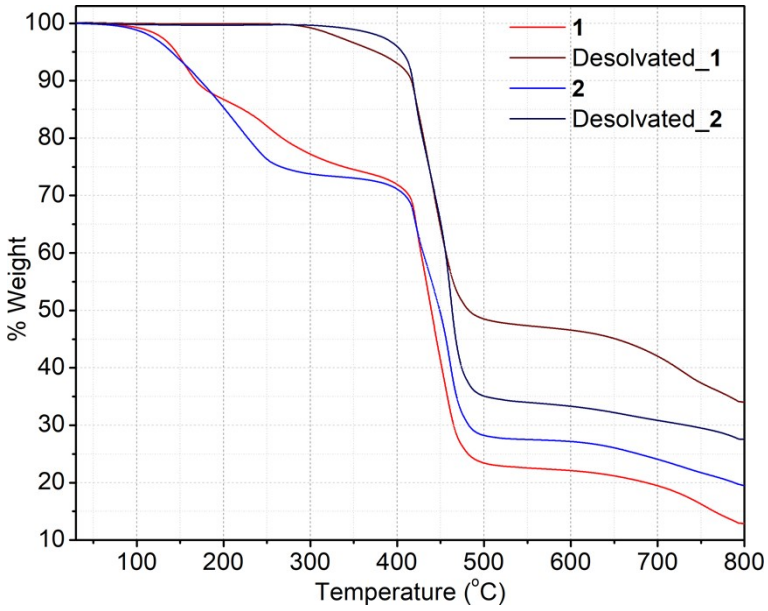

(*a*)

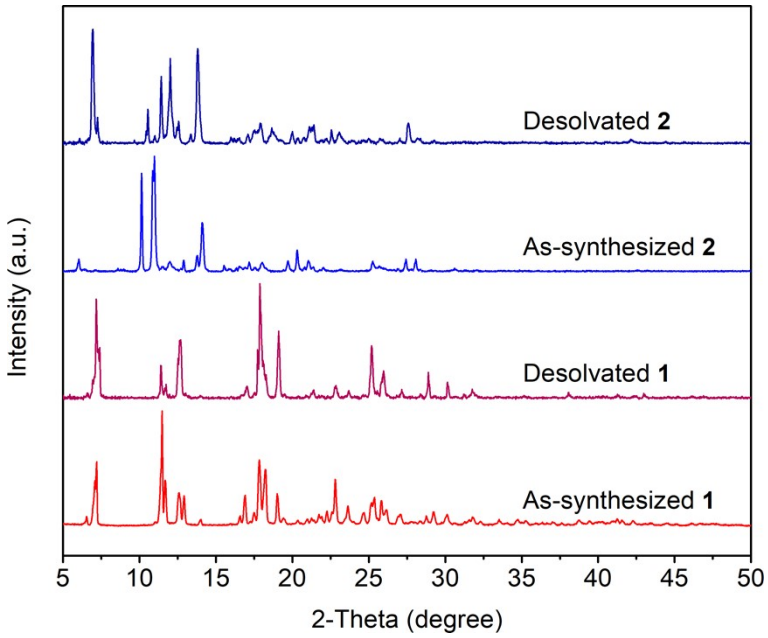

(*b*)

Fig. S6 (*a*) TGA curves of **1** and **2**, and (*b*) comparison of the room temperature PXRD patterns for **1** and **2** before and after the desolvation processes.

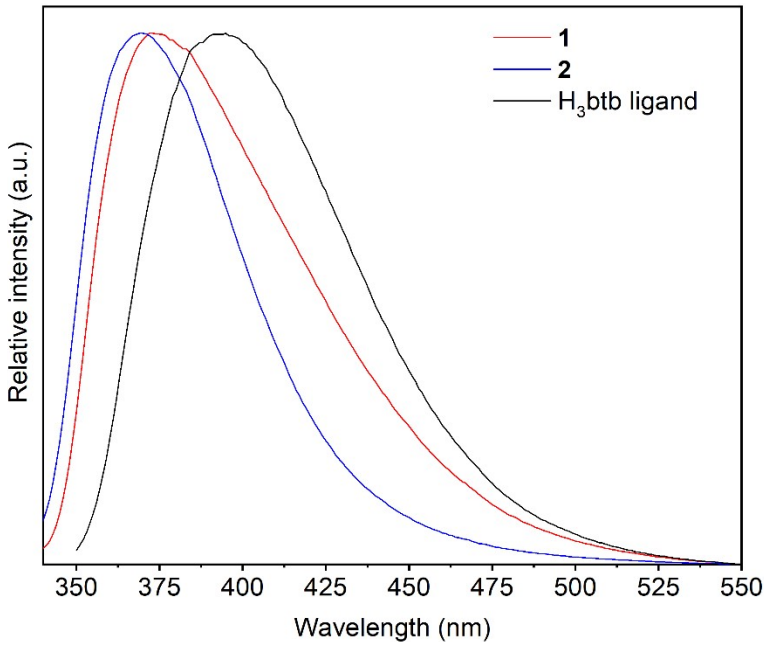

Fig. S7 Solid-state photoluminescence spectra of **1**, **2**, and H_3BTB at room temperature.

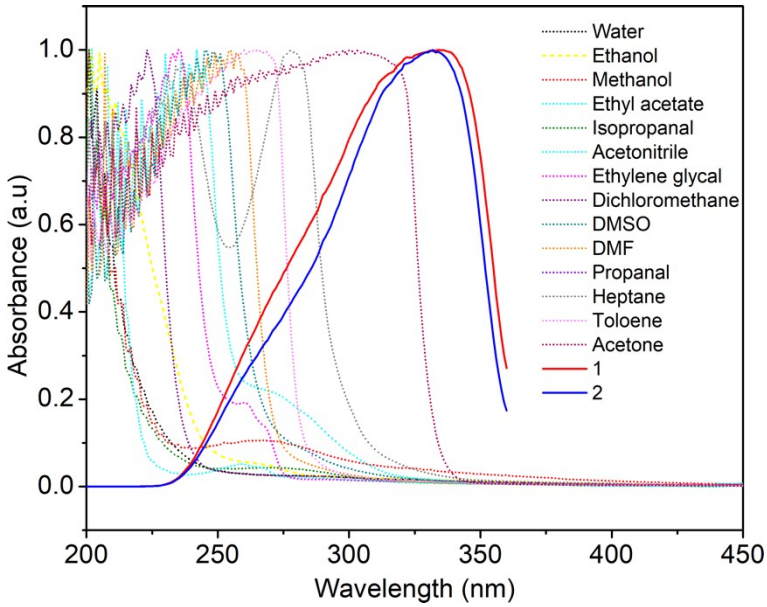

(*b*)

Fig. S8 The UV–vis absorbance spectra of water and various organic compounds together with excitation spectra of **1** and **2**.

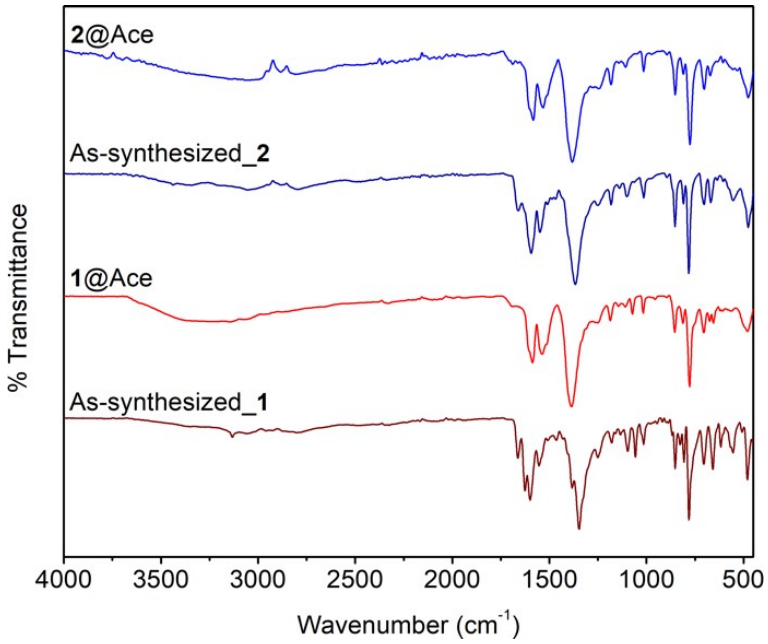

(*a*)

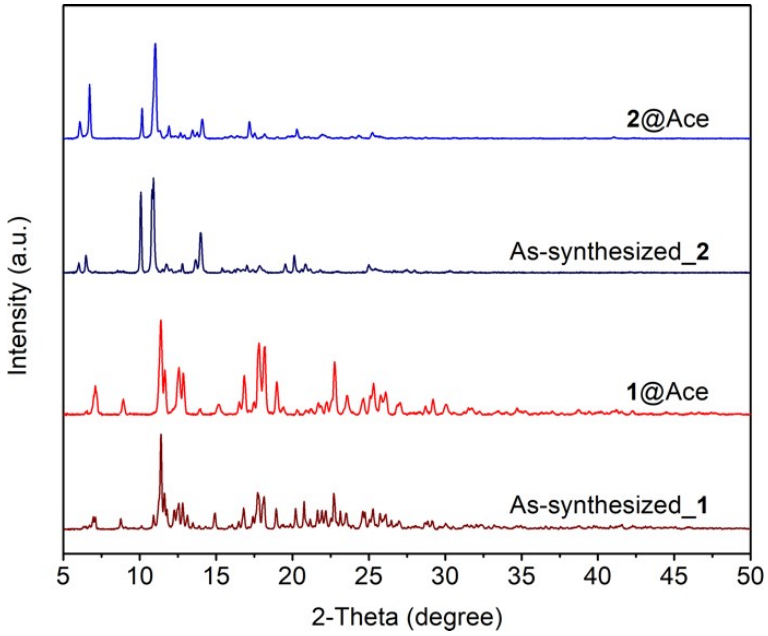

(*b*)

Fig. S9 (*a*) IR spectra and (*b*) PXRD patterns of **1** and **2** after soaking in acetone.

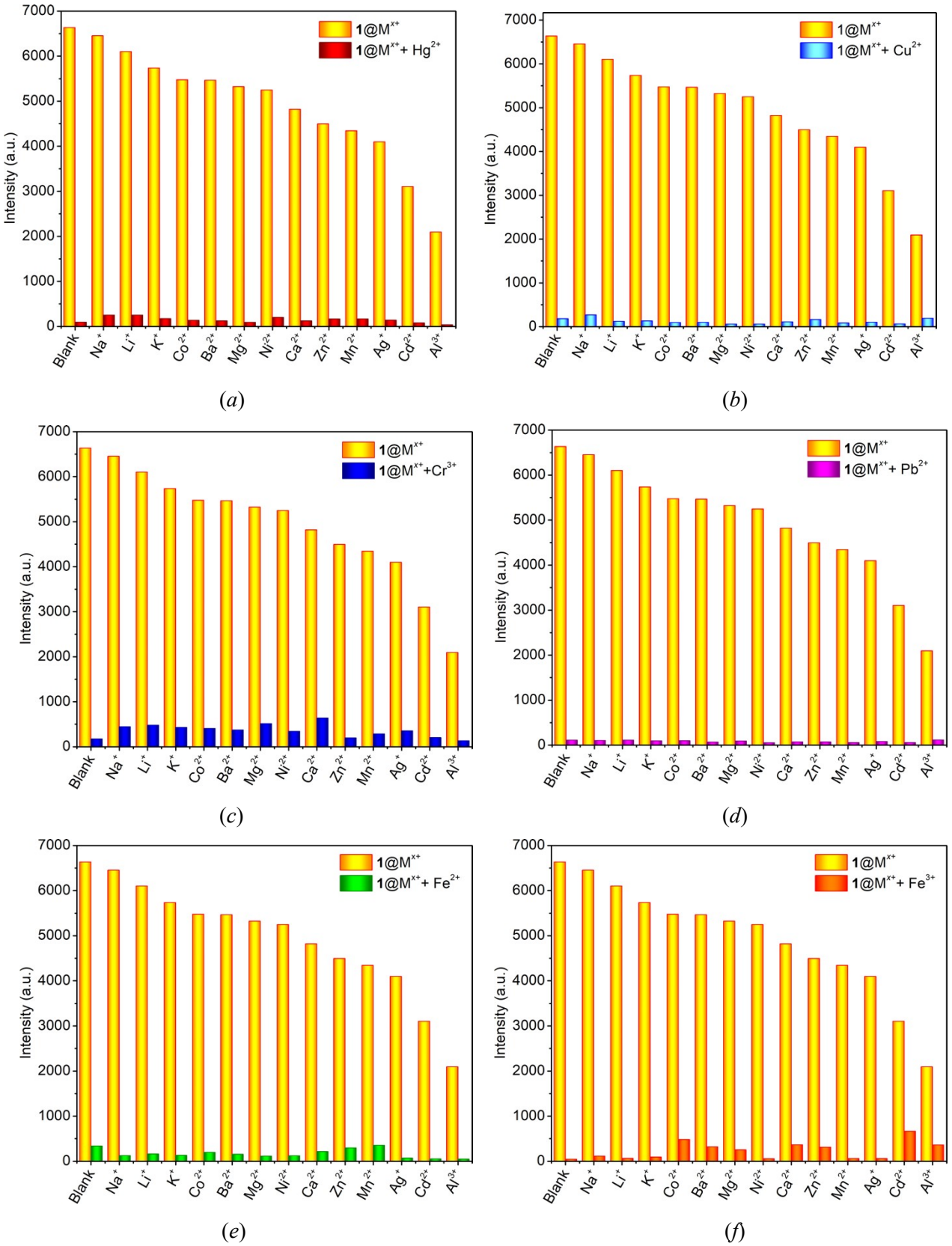

Fig. S10 Relative luminescence intensities of **1** dispersed in the aqueous solutions of individual metal ions (yellow columns) and the quenched luminescence intensities after the addition of (*a*) Hg^{2+}, (*b*) Cu^{2+}, (*c*) Cr^{3+}, (*d*) Pb^{2+}, (*e*) Fe^{2+}, and (*f*) Fe^{3+} ions.

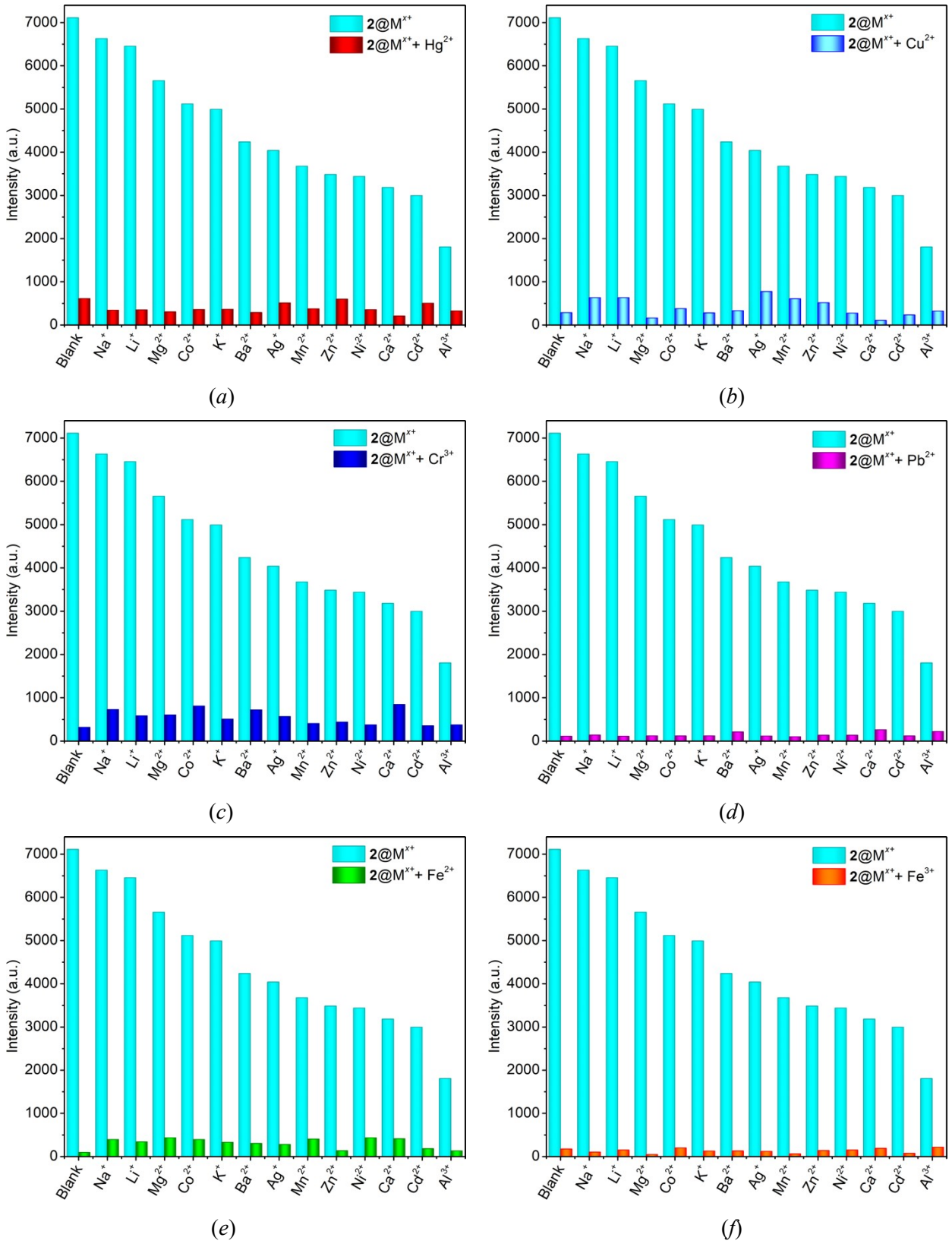

Fig. S11 Relative luminescence intensities of **2** dispersed in aqueous solutions of individual metal ions (turquoise columns) and the quenched luminescence intensities after the addition of (*a*) Hg^{2+}, (*b*) Cu^{2+}, (*c*) Cr^{3+}, (*d*) Pb^{2+}, (*e*) Fe^{2+}, and (*f*) Fe^{3+} ions.

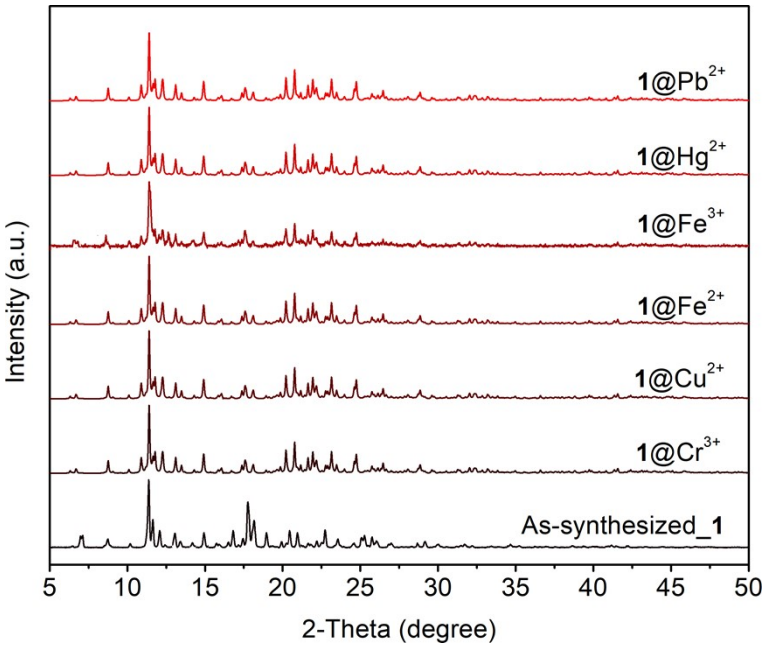

(*a*)

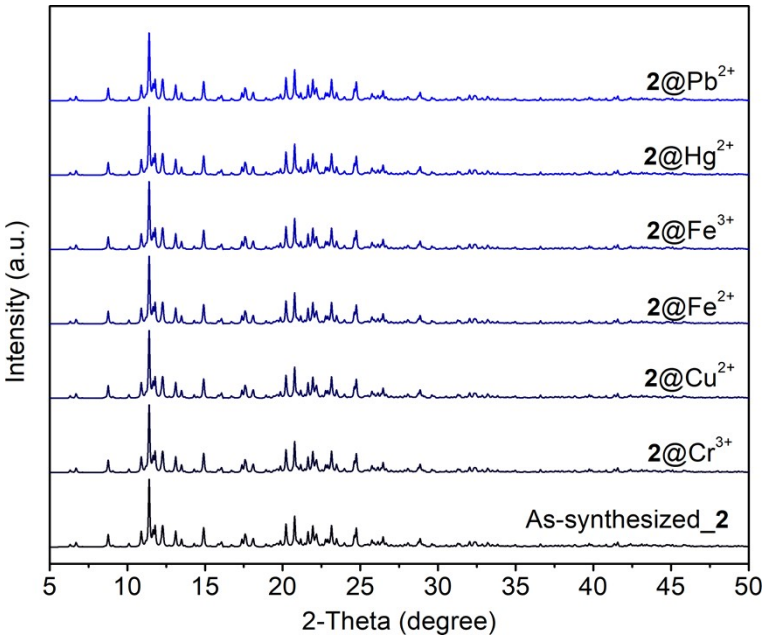

(*b*)

Fig. S12 PXRD patterns of (*a*) **1** and (*b*) **2** before and after the fluorescence quenching experiments.

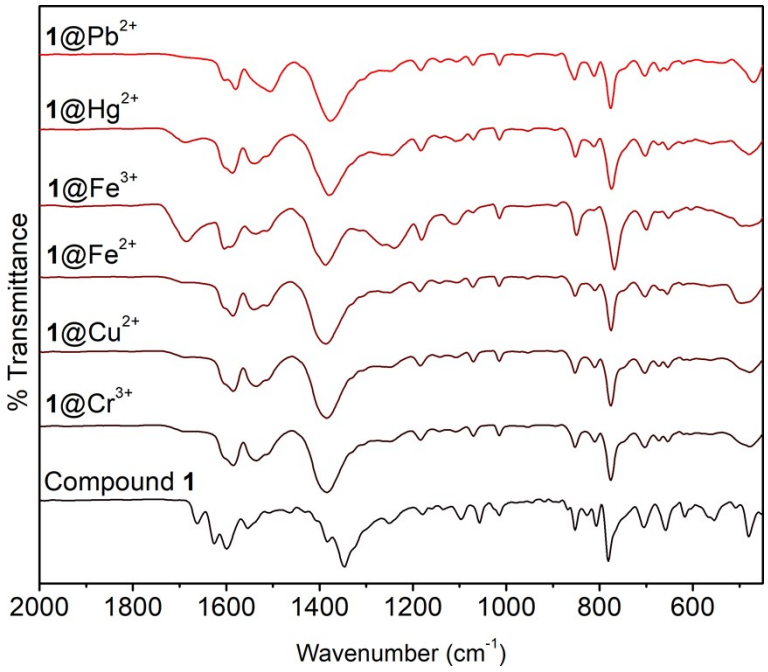

(*a*)

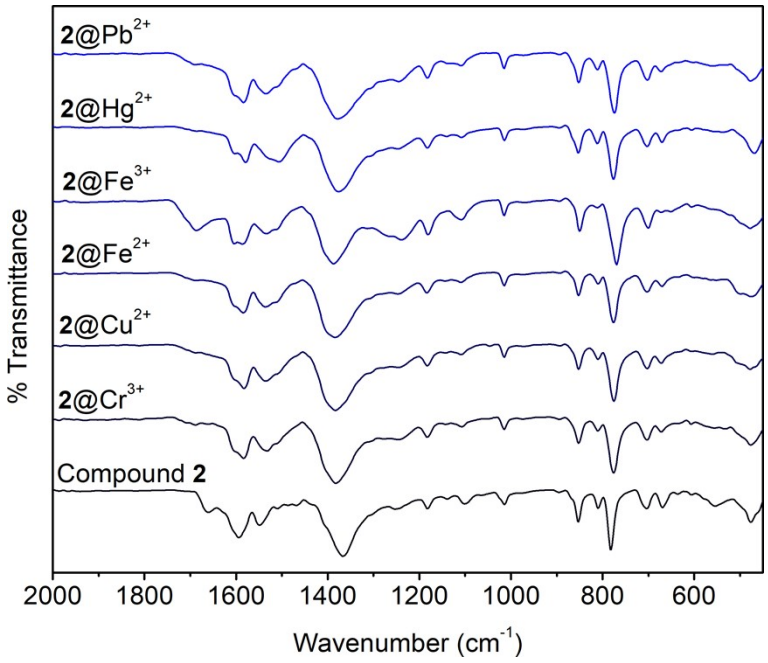

(*b*)

Fig. S13 IR spectra of (*a*) **1** and (*b*) **2** before and after the fluorescence quenching experiments.

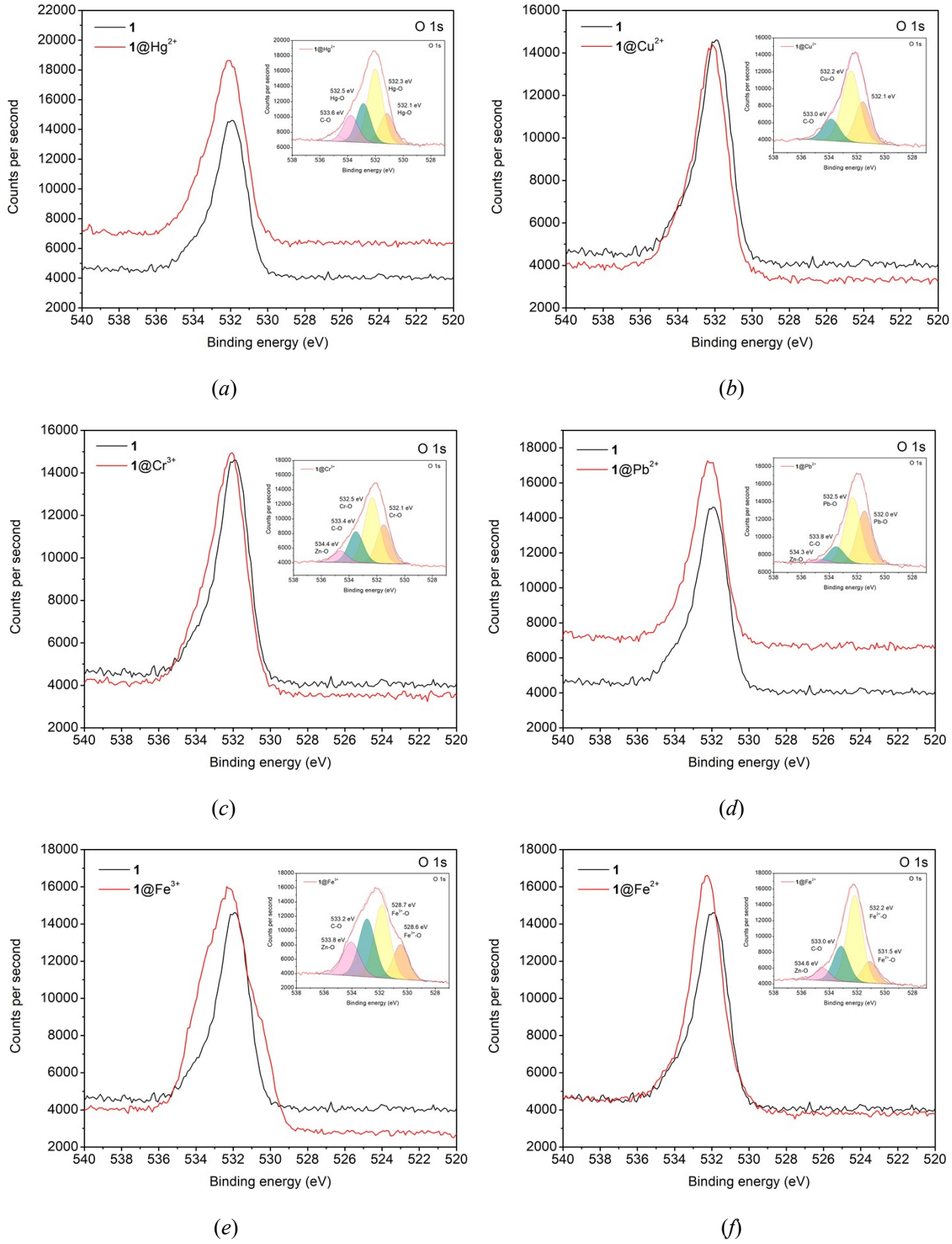

Fig. S14 High resolution XPS spectra of O 1s core levels of **1** (black) and its metal incorporated forms (red) (*a*) **1**@Hg^{2+}, (*b*) **1**@Cu^{2+}, (*c*) **1**@Cr^{3+}, (*d*) **1**@Pb^{2+}, (*e*) **1**@Fe^{3+}, and (*f*) **1**@Fe^{2+}.

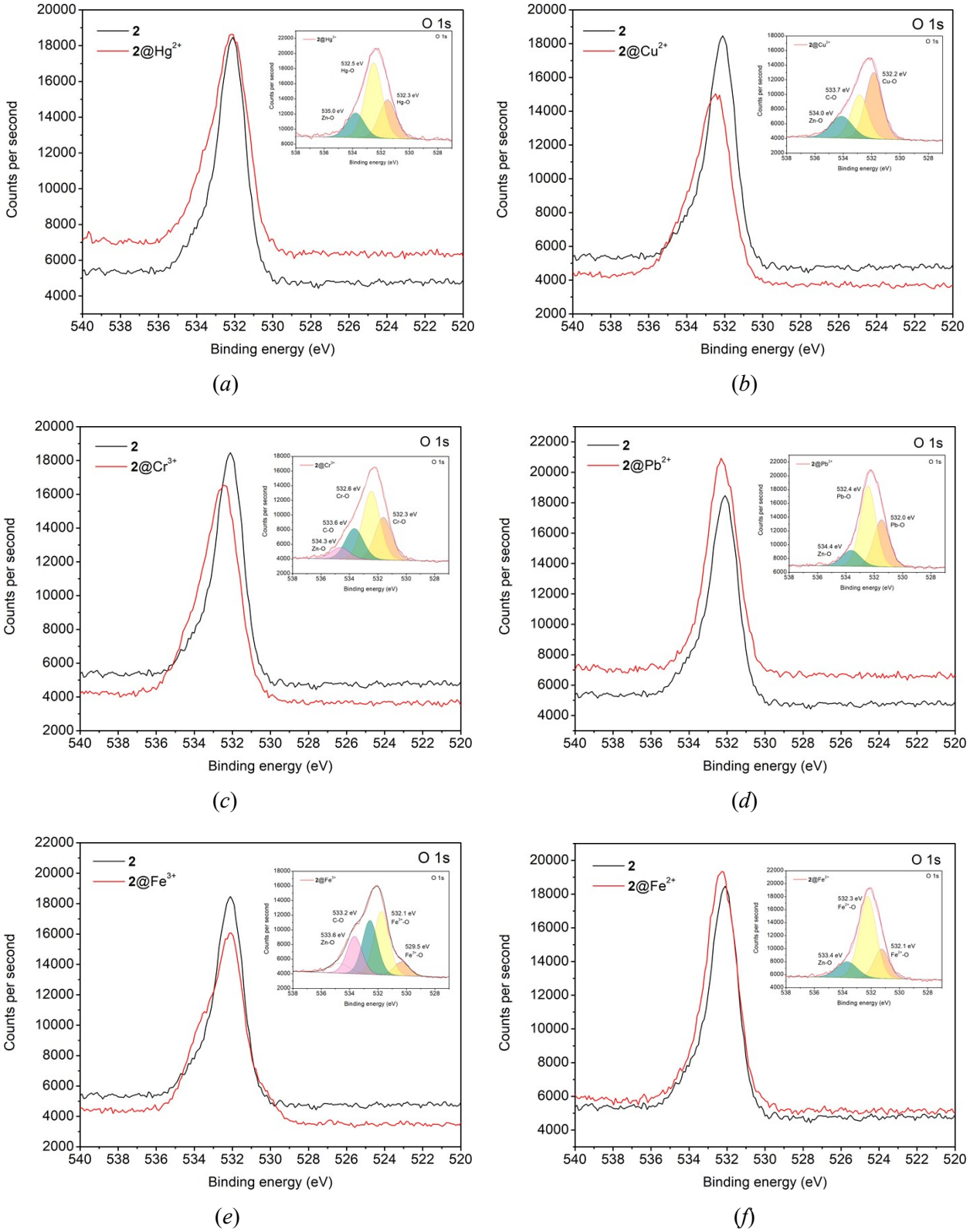

Fig. S15 High resolution XPS spectra of O 1s core levels of **2** (black) and its metal incorporated forms (red) (*a*) **2**@Hg^{2+}, (*b*) **2**@Cu^{2+}, (*c*) **2**@Cr^{3+}, (*d*) **2**@Pb^{2+}, (*e*) **2**@Fe^{3+}, and (*f*) **2**@Fe^{2+}.

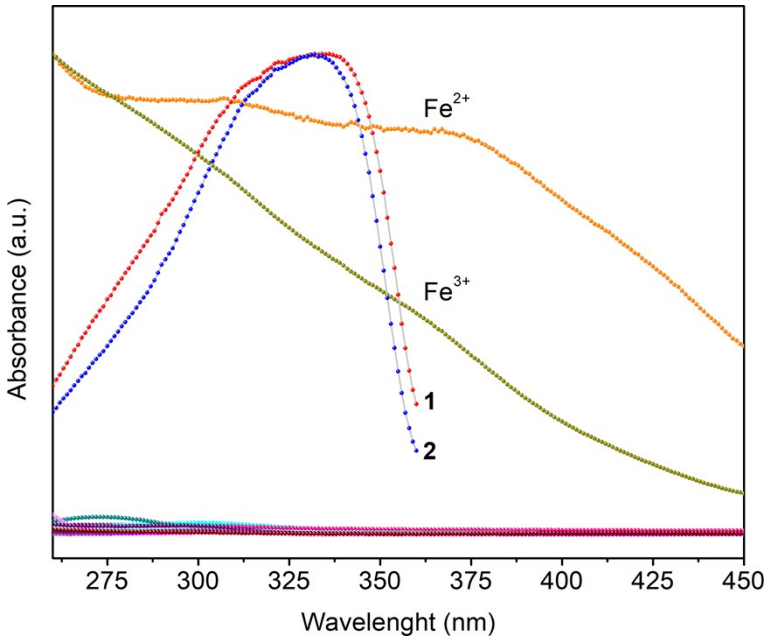

Fig. S16 The UV–vis absorbance spectra of aqueous solutions containing individual metal ions together with excitation spectra of **1** and **2**.

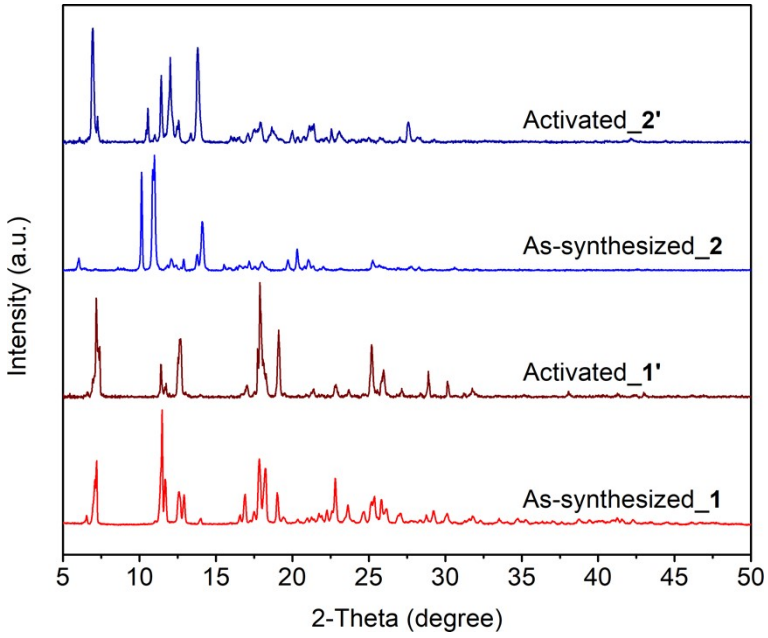

Fig. S17 Comparison PXRD patterns of the as-synthesized **1** and **2** and their activated samples **1**' and **2**'.

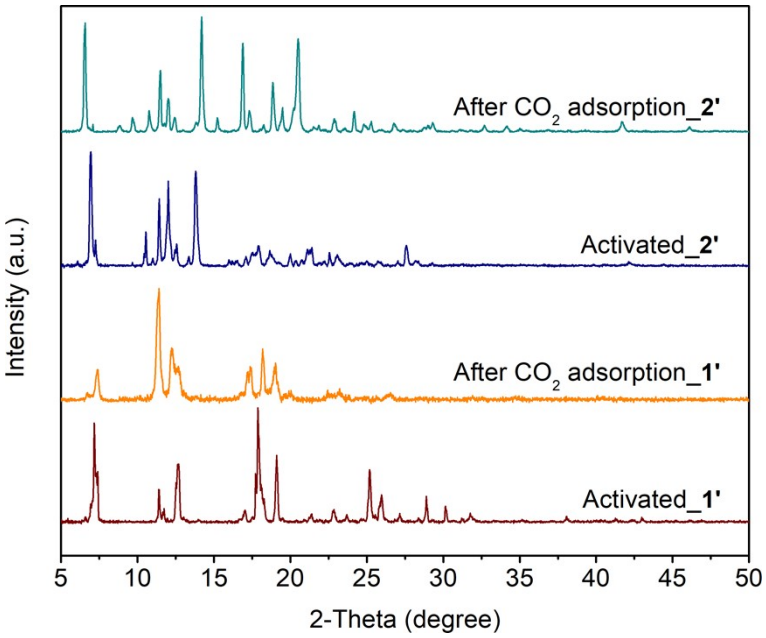

Fig. S18 Comparison PXRD patterns of activated **1'** and **2'** and those samples after high-pressure (up to 20 bar) CO_2 sorption at 338 K (65 °C).